

## FUNGI — ГРИБЫ

### Morphology and phylogeny of *Diderma aurantiacum* (Myxomycetes) — a new species for Russia from the Far East

V. I. Gmoshinskiy<sup>1</sup>, Yu. K. Novozhilov<sup>2</sup>, I. S. Prikhodko<sup>2</sup>, F. M. Bortnikov<sup>1</sup>,  
O. N. Shchepin<sup>2,3</sup>, M. Schnittler<sup>3</sup>

<sup>1</sup>Lomonosov Moscow State University, Moscow, Russia

<sup>2</sup>Komarov Botanical Institute of the Russian Academy of Sciences, St. Petersburg, Russia

<sup>3</sup>Institute of Botany and Landscape Ecology, Ernst Moritz Arndt University Greifswald, Greifswald, Germany

Corresponding author: V. I. Gmoshinskiy, rubisco@list.ru

**Abstract.** Two specimens of a rare species *Diderma aurantiacum* collected in the Sikhote-Alin Nature Reserve and the territory of the Land of the Leopard National Park (Primorye Territory, Russian Federation) were found during revision of the myxomycete collection of the Mycological herbarium of the Komarov Botanical Institute (LE). These specimens are the first records of this species outside the Japanese islands. *Diderma aurantiacum* is characterized by a thick cartilaginous peridium of dull orange color that breaks into petal-like fragments during dehiscence, a small hemispherical columella, weakly branched dark capillitial threads with pale tips, and warted spores with darker warts arranged in small groups. The color photographs of sporocarp structures and SEM images of spores and capillitium are published for the first time. The partial nucleotide sequences of nrSSU (18S rDNA) and EF1 $\alpha$  genes of specimens from the Russian Far East differed clearly from these of other *Diderma* species.

**Keywords:** Amoebozoa, Didymiaceae, *Leangium*, Physarales, illustrations, slime molds, phylogeny, Far East, Primorye Territory, Russia.

### Морфология и филогения *Diderma aurantiacum* (Мухомycetes) — нового вида для России с Дальнего Востока

В. И. Гмошинский<sup>1</sup>, Ю. К. Новожилов<sup>2</sup>, И. С. Приходько<sup>2</sup>, Ф. М. Бортников<sup>1</sup>,  
О. Н. Щепин<sup>2,3</sup>, М. Шниттлер<sup>3</sup>

<sup>1</sup>Московский государственный университет имени М. В. Ломоносова, Москва, Россия

<sup>2</sup>Ботанический институт им. В. Л. Комарова РАН, Санкт-Петербург, Россия

<sup>3</sup>Институт ботаники и ландшафтной экологии Грайфсвальдского университета, Грайфсвальд, Германия

Автор для переписки: В. И. Гмошинский, rubisco@list.ru

**Резюме.** В ходе ревизии коллекции миксомицетов Микологического гербария Ботанического института им. В. Л. Комарова РАН (LE) было обнаружено два образца редкого вида *Diderma aurantiacum*, собранные в Сихотэ-Алинском государственном заповеднике и в национальном парке «Земля Леопарда» (Приморский край, Дальний Восток России). Это первые

находки данного вида за пределами Японских островов. *Diderma aurantiacum* характеризуется плотным, хрящевидным тускло-оранжевым перидием, который растрескивается на звездчатые фрагменты при созревании, небольшой шаровидной колонкой, слабо ветвящимися темными нитями капиллиция со светлыми окончаниями и бородавчатыми спорами, бородавочки на поверхности которых формируют группы. Впервые приводятся цветные фотографии спорокарпов и структур капиллиция этого вида. Сравнение частичных нуклеотидных последовательностей генов nrSSU (18S rDNA) и EF1 $\alpha$  показало значительное отличие образцов с Дальнего Востока России от других представителей рода *Diderma*.

**Ключевые слова:** Амоебозоа, Didymiaceae, *Leangium*, Physarales, иллюстрации, слизевики, филогения, Дальний Восток, Приморский край, Россия.

The genus *Diderma* Pers. (Physarales, Didymiaceae), based on the type species *Diderma globosum* Pers., was described by Person in 1794. It is currently one of the largest genera of myxomycetes, numbering 87 species (Person, 1794; Lado, 2005–2023).

Its most characteristic features are dark-colored spores, the absence of lime in capillitial threads (very rarely some threads may contain several amorphous granules), and granulated lime in a one-, two- or three-layered peridium (Poulain *et al.*, 2011), which may form individual lime scales in some cases, e. g., *Diderma tigrinum* (Schrad.) Prikhodko *et al.* (Prikhodko *et al.*, 2023, syn. *Lepidoderma tigrinum* (Schrad.) Rostaf.).

The genus *Diderma* is usually divided into two subgenera: *Diderma* and *Leangium* Link (Poulain *et al.*, 2011). The subgenus *Diderma* is characterized by an outer peridium rich in lime, fragile, rough or smooth, often eggshell-like, rarely dehiscing stellately. The genus *Leangium* was described by H. F. Link (1809); its members were characterized by often stalked, almost globose sporangia, globose or hemispherical columella, thick cartilaginous peridium (structurally resembling peridium of *Leocarpus* Link), dehiscing in petal-like manner in certain species. Later, several species were transferred to the genus *Leangium*, and in 1899, T. Macbride proposed to move *Leangium* to the subgeneric level, *Diderma* subg. *Leangium* (Link) T. Macbr. (MacBride, 1899) to accommodate species with a three-layered peridium consisting of an inner membranous layer covered by a granuliferous lime and finally another organic layer. In some cases the third, organic layer is extremely thin and not clearly discernible.

More recent authors have pointed out that the limits between the subgenera *Leangium* and *Diderma* are poorly defined (Martin, Alexopoulos, 1969; Poulain *et al.*, 2011). Poulain *et al.* (2011) list the species that can be assigned to the subgenus *Leangium*: *Diderma antarcticum* (Speg.) Sturgis, *D. darjeelingense* K. S. Thind *et* H. S. Sehgal, *D. floriforme* (Bull.) Pers., *D. lucidum* Berk. *et* Broome, *D. ochraceum* Hoffm., *D. radiatum* (L.) Morgan, *D. roanense* (Rex) T. Macbr., *D. rufum* Nann.-Bremek., *D. rugosum* (Rex) T. Macbr., *D. sauteri* (Rostaf.) T. Macbr., *D. subasteroides* M. L. Farr, and *D. umbilicatum* Pers. Because of the stalked sporangia, cartilaginous peridium, and the presence of columella, this list can be extended: *Diderma aurantiacum* Y. Yamam. *et* Nann.-Bremek., *D. asteroides* (Lister *et* G. Lister) G. Lister, *D. cattienne* Novozh. *et* D. W. Mitch., *D. dalatense* Novozh., Prikhodko *et* Shchepin, *D. subasteroides* M. L. Farr., *D. velutinum* Bortnikov, and *Polyschismium trevelyanii* (Grev.) Corda

(≡ *Leangium trevelyanii* Grev.). The latter taxon belongs even to a different genus, as shown by a revision based on genetic investigations (Prikhodko *et al.*, 2023).

*Diderma aurantiacum* was described from Japan in 1990. The holotype, Y. Yamamoto 8738, from Mountain Shiraga is stored in The National Museum of Nature and Science (TNS) in Japan and the isotype is stored in the collection of Nannenga-Bremekamp no. 16.393 (Nannenga-Bremekamp, Yamamoto, 1990). In addition to the type locality, this species has been recorded in Sasaguri Forest of Kyushu University (Harakon *et al.*, 2005) and on the Izu Peninsula (Yano *et al.*, 2017). So far, all observations of this species have been made only in Japan.

During revision of myxomycetes collected in the Primorye Territory (Russia), two specimens of *Diderma aurantiacum* were found that agree in morphological features with the type description. In the present work, morphological features of this species are discussed, accompanied by the first color macro- and microphotographs and sequences of four genetic markers: nrSSU (18S rDNA), EF1 $\alpha$ , COI, and mtSSU.

## Materials and Methods

### Morphological studies

Photographs of sporocarps were taken with a ZEISS Axio Zoom.V16 dissecting microscope and a Micromed 3 var. 3LED light microscope equipped with a E3CMOS06300 digital camera and epi-illumination. Series of pictures were taken in different optical sections and processed using Helicon Focus ver. 6.0.18. The dimensions of spores, capillitium, and sporocarps were calculated using ToupView 3.7 and ImageJ ver. 1.52a.

Microscopic measurements and photographs were made with a ZEISS Axio Imager.A1 light microscope with differential contrast using Zeiss Zen 3.2 software (Carl Zeiss Microscopy GmbH, free license, blue edition) software and Micromed 3 var. 3LED equipped with a E3CMOS06300 digital camera. For microscopy, sporocarps were mounted in polyvinyl-lactophenol or 4% KOH. The spore surface and structure of capillitium were studied using Jeol JSM-6380 LA (Jeol, Tokyo, Japan) and Quattro S (Thermo Fisher Scientific, Waltham, MA, USA) scanning electron microscopes. Specimens for SEM were mounted on copper stubs with nail polish and sputter-coated with gold-palladium.

### DNA extraction, amplification, and sequencing

Extraction of genomic DNA was performed from mature air-dried fruiting bodies without a trace of fungal contamination. Approximately 2–5 sporocarps were placed in 2 ml safe-lock tubes with addition of steel or ceramic balls 3 mm diam. and frozen at –20 °C for at least 30 min. Afterwards, samples were crushed in a Bioprep-24 homogenizer (Hangzhou Allsheng Instruments, Hangzhou, China). DNA was extracted either with a PhytoSorb kit (Sintol, Moscow, Russia) according to the manufacturer's protocol with minor modifications (the spore homogenate was eluted with 450  $\mu$ l of extraction buffer; lysis buffer was added without preliminary precipitation step and supernatant transfer into a new sterile tube; final elution volume was 80–100  $\mu$ l) or

with a MagPure Plant DNA Kit (Magen Biotechnology, Guangzhou, China) according to the manufacturer’s protocol.

To reconstruct the phylogeny, two unlinked genetic markers were sequenced. The first part of nrSSU (nuclear 18S rRNA gene), which is free of introns, was obtained with the S2 forward primer (Fiore-Donno *et al.*, 2008) and SU19R or SSU\_rev reverse primers (Fiore-Donno *et al.*, 2011; Prikhodko *et al.*, 2023). A fragment of translation elongation factor 1-alpha (EF1 $\alpha$ ) gene was amplified using a PB1F/PB1R primer pair (Novozhilov *et al.*, 2013). In addition, partial sequences of cytochrome c oxidase subunit 1 gene (COI) and mitochondrial 16S rRNA gene (mtSSU) were obtained from two samples of *Diderma aurantiacum*. COI was amplified and sequenced with a COMF/COMRs primer pair (Liu *et al.*, 2015; Novozhilov *et al.*, 2019) and mtSSU with a Kmit\_F/Kmit\_R primer pair (Lado *et al.*, 2022).

A list of primers, their sequences, and amplification protocols for different primer combinations are provided in Table 1.

Table 1

**Primer pairs and amplification protocols used in this study**

Name	F/R	Sequence (5’-3’)	Amplification protocol
S2	F	TGGTTGATCCTGCCAGTAGTGT	5 min at 95 °C, 36 cycles (30 sec at 95 °C, 20 sec at 56 °C, 50 sec at 72 °C) and 5 min at 72 °C
SU19R	R	GACTTGTCCTCTAATTGTTACTCG	
SSU_rev	R	AGACTTGTCCCTCYAATTGTTAC	
PB1F	F	ACCCGTGAGCACGCTCTCCT	5 min at 95 °C, 36 cycles (30 sec at 95 °C, 30 sec at 65.4 °C, 1 min at 72 °C) and 10 min at 72 °C
PB1R	R	CGCACATGGGCTTGGAGGGG	
COMF	F	GCTCCTGATATGGCWTTTC	5 min at 95 °C, 36 cycles (30 sec at 95 °C, 20 sec at 52 °C, 1 min at 72 °C) and 10 min at 72 °C
COMRs	R	CATGRAAWGCATATCWARACC	
Kmit_F	F	AGTGTTATTCGTGATGACTGG	5 min at 95 °C, 32 cycles (30 sec at 95 °C, 1 min at 52 °C, 90 sec at 72 °C) and 10 min at 72 °C
Kmit_R	R	CGAATTAACCACATCTCCACC	

PCR reactions were prepared with 10  $\mu$ l of 2  $\times$  BioMaster HS-Taq PCR-Color reaction mix (Biolabmix, Novosibirsk, Russia) containing 100 mM KCl, 0.4 mM dNTPs, 4 mM MgCl<sub>2</sub>, 0.06 U/ $\mu$ l TaqDNA polymerase, 0.2% Tween20, and several dyes (xylene cyanol, bromophenol blue, Orange G, and tartrazine) with addition of 3 nmol of each primer, 1–3  $\mu$ l of template DNA, and diH<sub>2</sub>O up to a total volume of 20  $\mu$ l. The amplification was carried out with a C1000 Touch (Bio-Rad, Hercules, USA) thermal cycler. Products of amplification were stained with SYBR Green I (Lumiprobe, Moscow, Russia), separated by 1.2% agarose gel electrophoresis, observed in a Gel Doc XR+ System (Bio-Rad, Hercules, USA), and then purified using

a CleanMag DNA (Evrogen, Moscow, Russia) purification kit before PCR or sequencing with a BrilliantDye Terminator v3.1 Cycle Sequencing Kit (NimaGen, Nijmegen, the Netherlands) using the primers mentioned earlier. Sequencing products were purified with a NimaGen D-Pure DyeTerminator Cleanup kit and analyzed on an ABI 3500 automated DNA sequencer (Applied Biosystems, Foster City, USA) equipped with a standard 50 cm capillary array.

### Alignments, model selection, and phylogenetic analyses

The newly obtained nrSSU and EF1 $\alpha$  sequences were edited and assembled into two single gene alignments in Unipro UGENE (Okonechnikov *et al.*, 2012) with the sequences deposited in NCBI GenBank. The final alignments were generated using MAFFT v7.496 online service (Katoh, Standley, 2013; Katoh *et al.*, 2019) with E-INS-I option for nrSSU and G-INS-i option for EF1 $\alpha$  with default gap penalties. Exon parts of EF1 $\alpha$  sequences were determined according to the known EF1 $\alpha$  protein and nucleotide sequences of *Meriderma carestiae* (Ces. et De Not.) Mar. Mey. et Pou-lain (GenBank MH460968; Fiore-Donno *et al.*, 2019) and *Diderma tigrinum* (GenBank EF513195; Fiore-Donno *et al.*, 2010).

After manual editing and trimming of the primer sequences, two sets of nucleotide sequences were merged into a single alignment with two partitions using SequenceMatrix 1.8. (Vaidya *et al.*, 2011). Maximum likelihood (ML) analyses were performed using IQ-TREE 1.6.12 (the last stable release; Nguyen *et al.*, 2015) launched on the local machine. The TIM2e+I+G4 evolutionary model was selected for nrSSU partition and TN+F+I+G4 for EF1 $\alpha$  partition according to the ModelFinder tool implemented in IQ-TREE (Kalyaanamoorthy *et al.*, 2017). 1000 ultrafast bootstrap (UBS) replicates (Hoang *et al.*, 2018) were performed to obtain confidence values for the branches. Bayesian inference (BI) was performed with the same dataset using MrBayes 3.2.7a (Huelsenbeck, Ronquist, 2001) run on CIPRES Science Gateway (Miller *et al.*, 2010). The phylogenetic analysis was run four times as four separate chains for  $10 \times 10^6$  generations (sampling every 1000). The convergence of MCMC chains was estimated using Tracer 1.7.2 (Rambaut *et al.*, 2018) and by the average standard deviation of split frequencies; based on the estimates, the first 25% generations were discarded as burn-in. Posterior probabilities (PP) for clades were exported to the ML-tree. Phylogenetic tree with combined supports was visualized using FigTree 1.4.4 and edited using CorelDRAW 24.0.

### Data Availability

The DNA sequences generated during the current study are available in NCBI GenBank. The list of specimens used in the phylogenetic reconstruction is available as [Supplementary material](#)<sup>1</sup>, and together with concatenated alignment, partition file, and phylogenetic tree in the Newick format can also be found in Supplementary materials on FigShare: <https://doi.org/10.6084/m9.figshare.21972989>.

<sup>1</sup> Electronic supplement is available at the end of the article page on the journal website (<https://doi.org/10.31111/nsnr/2023.57.1.27>).

### Specimens examined

*Diderma aurantiacum*. **Russia**, Primorye Territory, Nadezhdinsky District, Land of the Leopard National Park, 43.40442°N, 131.54481°E, mixed damp polydominant forest with *Acer mono* Maxim., *Pinus koraiensis* Siebold et Zucc., *Abies holophylla* Maxim., *A. nephrolepis* (Trautv. ex Maxim.) Maxim., on the upper side of a dead log of *Abies* sp. completely covered by mosses, 3 IX 2011, *Novozhilov*, LE 286478; Terneysky District, Sikhote-Alin Nature Reserve, near the Yasnaya river, 45.23789°N, 136.49733°E, mixed forest with *Quercus mongolica* Fisch. ex Turcz., *Betula davurica* Pall., *B. platyphylla* Sukaczew, and *Larix gmelinii* (Rupr.) Kuzen., on dead wood of *Larix gmelinii*, 31 VIII 2014, *Novozhilov*, *Shchepin*, *D. A. Erastova*, *Schnittler*, LE 302633 [was previously mentioned as *Diderma* cf. *floriforme* (*Novozhilov et al.*, 2017: fig. 8, 9)].

*Diderma asteroides*. **Russia**, Pskov Region, Bejanitskiy District, Polistovskiy Natural State Reserve, 57.10401°N, 30.37171°E, forest of black alder (*Alnus glutinosa* (L.) Gaertn.) with *Betula pendula* Roth and *Sorbus aucuparia* L., on the edge of a bog, on the upper side of dead leaf of *Alnus glutinosa*, 6 XI 2019, *Gmshinskiy*, *A. V. Matveev*, *N. I. Borzov*, MYX 12440.

*Diderma floriforme*. **Russia**, Moscow Region, Serpukhovskiy District, Prioksko-Terrasny Natural State Biosphere Reserve, 54.88105°N, 37.65570°E, mixed polydominant forest with *Quercus robur* L., *Picea abies* (L.) H. Karst., *Tilia cordata* Mill., *Pinus sylvestris* L., on the downside of a dead log, 21 X 2021, *Gmshinskiy*, *N. I. Kireeva*, MYX 18793; **Ukraine**, Kiev Region, Bucha District, 50.58390°N, 30.00869°E, in the hollow of an *Quercus robur* stump, 27 VIII 1917, *M. Zelle*, LEP 547.

*Diderma radiatum*. **Russia**, Tver Region, Nelidovsky District, Central Forest Natural State Biosphere Reserve, 56.47230°N, 32.99247°E, mixed, swamped forest with *Picea abies*, *Betula pendula*, *Sorbus aucuparia*, with a continuous covering of *Sphagnum* spp. on ground, on downside of dead deciduous log, 16 X 2016, *Gmshinskiy*, *N. I. Kireeva*, MYX 8903; *ibid.*, 56.46725°N, 32.95655°E, spruce forest (*Picea abies*), with mixture of *Betula pendula* and *Populus tremula*, on dead log of conifer tree, 4 XI 2017, *Gmshinskiy*, *N. Yu. Buchtayarova*, MYX 9071; *ibid.*, 4 XI 2017, *Gmshinskiy*, *N. Yu. Buchtayarova*, MYX 9084.

## Results and Discussion

*Diderma aurantiacum* Y. Yamam. et Nann.-Bremek., 1990, in Nannenga-Bremekamp et Yamamoto, Proc. Kon. Ned. Akad. Wetensch. 93(3): 267. (Figs. 1, 2)

Sporocarps scattered (Fig. 1A), stalked or rarely almost sessile, 0.85–1.1 mm in total height. Sporotheca subglobose or slightly flattened, usually yellow to dull orange (Fig. 1A, B, C), yellowish-brown to brown when lacking lime (Fig. 1D, E, G, H), 0.45–0.8 × 0.4–0.7 mm. Hypothallus membranous, pale brown, discoid, individual. Stalk either normally developed, half or more than a half of the total height (up to 0.6 mm), rugose, pale brown (Fig. 1B, D, E), or almost absent and replaced by expanded hypothallus (Fig. 1H), darker near the base, widening in the upper part and gradually becoming the base of sporotheca (Fig. 1B, D, E). Peridium double, with closely appressed layers (Fig. 2E); outer layer cartilaginous, consists of tightly packed dull orange lime granules, if normally developed. Inner layer membranous (Fig. 2E, see arrow), translucent, pale brownish (Fig. 1A, B). In case of a poorly developed outer layer the peridium looks brown because of the spore mass showing through (Fig. 1D, E, G, H). Dehiscence apical, irregular to mostly flori-form (Fig. 1A–D). Columella hemispherical to subglobose or globose, reaching one-third or a little more of the sporotheca height, yellow-brown, rugose (Fig. 1C, I).



Fig. 1. *Diderma aurantiacum* (A, B, D, G, H – from LE 302633; C, E, F, I – from LE 286478). A–C – mature dehiscent sporangia; D, E – dehiscent and intact sporangia with limeless peridium; F – capillitium with hyaline tips; G, H – stalked and short-stalked sporangia with aberrant development of outer peridium (dull yellow lime grains are visible); I – destroyed sporangium with exposed columella. Scale bars: A–E, H – 500  $\mu\text{m}$ ; F, G, I – 200  $\mu\text{m}$ .

Capillitium radiating from the columella, but loosely attached to it, composed of almost smooth threads (about 2  $\mu\text{m}$  diam.), sometimes with several dark node-like thickenings up to 5  $\mu\text{m}$  diam. (Fig. 2A, B), dark brown in both reflected and transmitted light excluding the hyaline tips (Fig. 1F), sparingly branched (Fig. 2A, I),

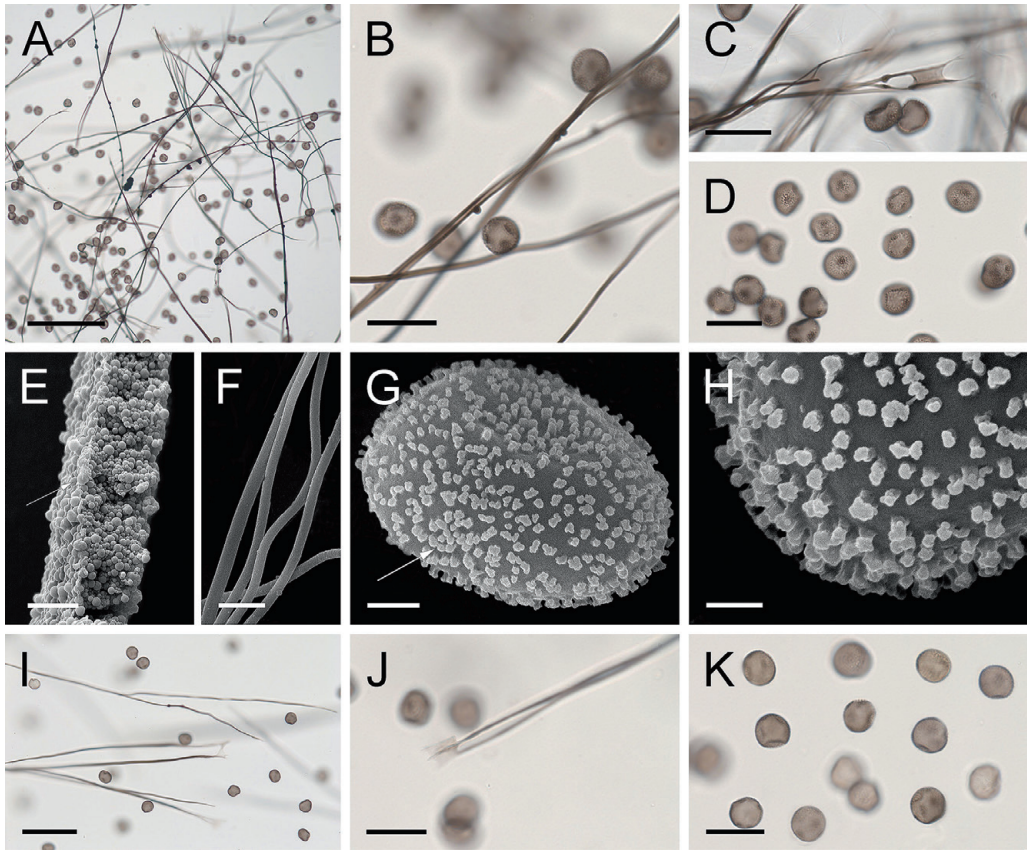


Fig. 2. Capillitium and spores of *Diderma aurantiacum*  
(A–G – from LE 302663; H–K – from LE 286478).

A–D, I–K – capillitium and spores in transmitted light (TL) (C, I, J – H-shaped ends of capillitium); E – section of the peridium; the arrow points to the inner membranous layer; F–H – capillitium and spores in scanning electron microscopy (SEM); the arrow points to the group of warts.

Scale bars: A – 100 μm; B, C, D, J, K – 20 μm; E, F – 5 μm; G – 2 μm; H – 1 μm; I – 50 μm.

anastomosing only in the upper part and forming small light H-shaped expansions (Fig. 2C, I, J). Under SEM, capillitial threads almost smooth (Fig. 2F), occasionally with small, irregularly distributed, amorphous nodules. Spores dark brown in mass, dark purple-brown in transmitted light, globose,  $(10.1)11.0\text{--}12.1(12.7)$  μm diam. (mean = 11.6, SD = 0.57, n = 110), with uniformly thickened wall, densely warted, with 2–3 groups of darker warts on the visible part of the spore (Fig. 2D, K). Under SEM, spores are ornamented with irregularly distributed baculae with small nodules at the apices, giving them a coralloid appearance (Fig. 2G, H). Plasmodium unknown.

The most distinctive features of *Diderma aurantiacum* are dull orange to yellow-brown sporangia breaking into curling petal-like fragments of peridium, almost

non-branched, nearly smooth capillitial threads loosely attached to a yellowish-brown spherical columella, and warted spores with darker warts assembled in small groups.

The studied specimens of *Diderma aurantiacum* were identical in morphological features, although spore size was slightly different: LE 302633 — (10.1)10.8–11.9(12.5)  $\mu\text{m}$  (mean = 11.3, SD = 0.55, n = 55); LE 286478 — (10.6)11.4–12.3(12.7)  $\mu\text{m}$  (mean = 11.8, SD = 0.46, n = 55). They generally agree with the original description, but slightly differ in some details and complement it (Nannenga-Bremekamp, Yamamoto, 1990).

Sporangia of specimens from the Russian Far East were somewhat shorter than in the original description: 0.85–1 mm vs. 1.5 mm. The publication of Nannenga-Bremekamp and Yamamoto (1990: Fig. 2A) depicts two sporangia about 0.9–1.0 mm high, according to the scale bar. The original description states, “Columella slightly clavate, mostly filled with lime globules, reaching halfway or a little more in sporangium”, but the color of columella is not specified. However, the columella height is at most 40% of the sporangium diameter (Nannenga-Bremekamp, Yamamoto, 1990: Fig. 2B), which agrees with our observations: the columella also took up about 40% of the sporangium, was slightly narrowed at the base and colored like the inner peridium in yellowish-brown. The capillitium structure of studied specimens from the Russian Far East also corresponded to the type description: threads were “...rather simple, sparingly branched, inter-connected only near the tips by pale, small membranes”. The only difference was the presence of a large number of dark nodules scattered throughout the capillitium, which was unambiguously illustrated by Yamamoto (1998: 264, Fig. 2C). In the drawing, several dark nodular thickenings are clearly visible, but in our case, they were more numerous and sometimes larger. The original description states that the spores are “minutely warty”, while it is clearly shown that warts are not evenly arranged and small groups of darker warts are present (Nannenga-Bremekamp, Yamamoto, 1990: Fig. 2D). A similar spore ornamentation is depicted by Yamamoto (1998: 264, Fig. D). Spores of our specimens were warted with clearly visible separate groups of darker and thicker warts (Fig. 2B, D, J, K). The protologue indicates that the holotype was recorded on rotten wood. Both specimens studied herein also developed on dead wood of conifers (LE 302633 on *Larix gmelinii* and LE 286478 on *Abies* sp.).

In general, we believe that the fully formed sporangia of our specimens correspond to the protologue despite small differences. However, it should be noted that the studied specimens (especially LE 302633) had, in addition to normal sporocarps, a great number of those that developed with a deficiency of lime, so that their peridium was not yellowish, but brown (sometimes with separate grains of yellow lime, see Fig. 1G, H). Some of these sporocarps were also very short-stalked (Fig. 1H).

*Diderma aurantiacum* appears close to other species of the subgenus *Leangium*, e. g., *Diderma asteroids*, *D. cattense*, *D. floriforme*, *D. radiatum*, *D. roanense*, and *D. subasteroides*. However, there are notable differences supporting *D. aurantiacum* as a separate species. The typical morphological form of *D. floriforme* has a pearl grey to greyish

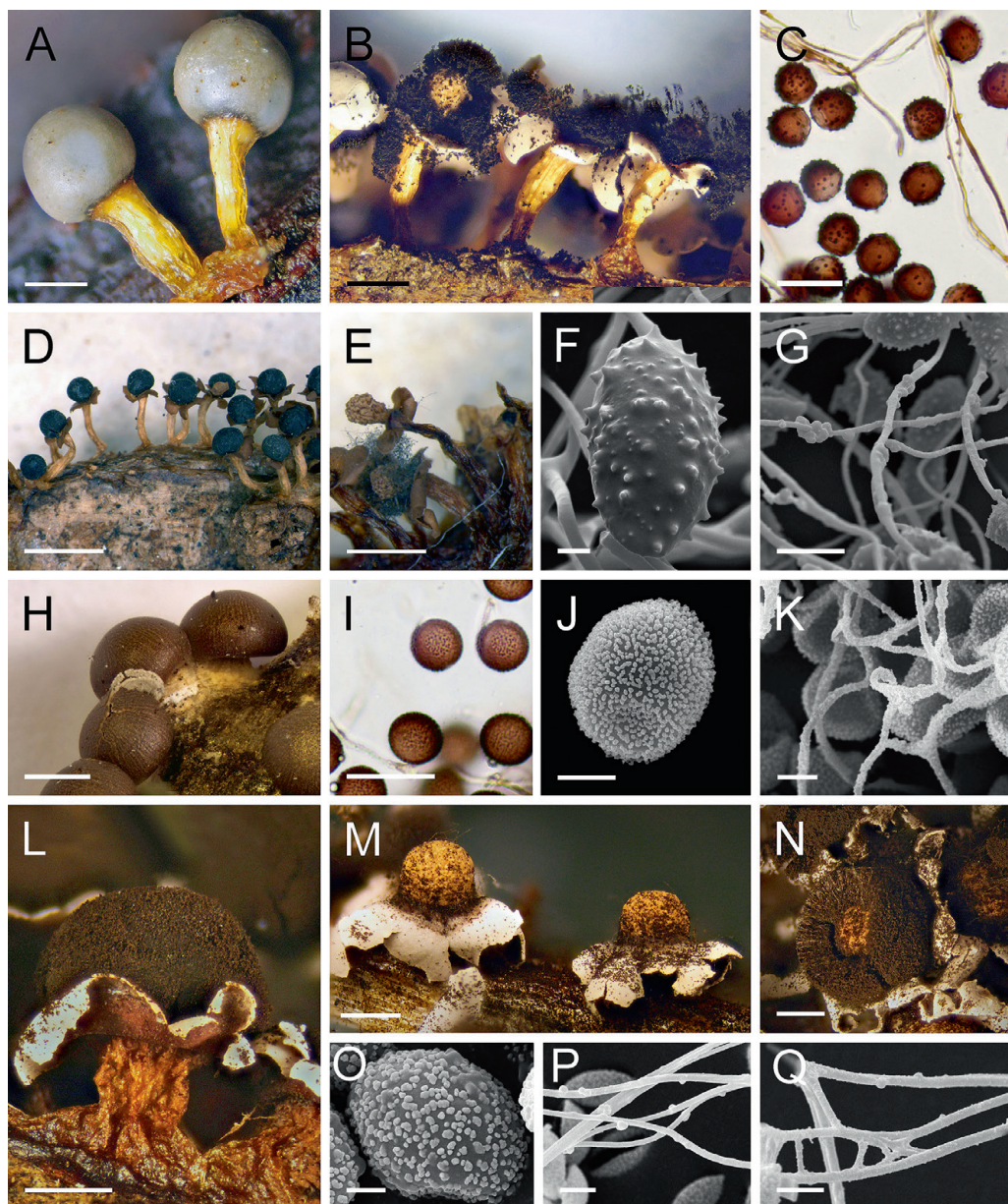


Fig. 3. *Diderma floriforme* (A–C, F–G – from MYX 18793, D–E – from LEP 547),  
*D. asteroides* (H–K – from MYX 12440), and *D. radiatum*  
(L – from MYX 8903, M – from MYX 9084, N–Q – from MYX 9071).

A, B, D, E – mature sporangia before and after dehiscence (E – club-shaped columella is visible);  
C, I – spores and capillitium (TL); F, G, J, K, O–Q – spore and capillitium (SEM); H – sporangia;  
L–N – mature sporangia.

Scale bars: A, B, H, L, M, N – 500  $\mu$ m; C, I – 20  $\mu$ m; D – 2 mm; E – 1 mm; F, O – 2  $\mu$ m; G – 10  $\mu$ m;  
J, K, P, Q – 5  $\mu$ m.

beige sporotheca (Fig. 3A, B, D), clavate columella (Fig. 3E), and spores with unevenly thickened wall and large, dark, scattered warts (Fig. 3C, F) (see also Martin, Alexopoulos 1969). Furthermore, sporangia of *D. floriforme* are usually aggregated in dense groups (Fig. 3B, D), while *D. aurantiacum* develops sporangia scattered over the substrate (Fig. 1A). *Diderma subasteroides* differs in flattened or discoid brown sporangia, poorly developed columella, abundantly branched capillitial threads, and larger spores reaching 12–13  $\mu\text{m}$  diam. (Farr, 1971). *Diderma asteroides* differs in brown peridium, hemispherical to subdiscoid sporangia (Fig. 3H), larger spores (12–13  $\mu\text{m}$ ) (Fig. 3I, J), abundantly branched capillitial threads (Fig. 3K), and flattened, whitish or pale flesh-colored columella (Lister, Lister, 1911; Martin, Alexopoulos, 1969). *Diderma radiatum* can be distinguished by its peridium, which is brown or reddish-brown on the outside (Fig. 3L) and white on the inside (Fig. 3M, N), short, stout stalks, and a large, pad-like columella occupying up to one-half of the sporotheca (Fig. 3M, N). In addition, the average sporangia of *D. radiatum* are much larger than those of *D. aurantiacum* — 0.6–1.4 mm vs. 0.4–0.8 mm (Nannenga-Bremekamp, 1968; Martin, Alexopoulos, 1969).

Another two species of the subgenus *Leangium*, *Diderma cattense* and *D. roanense*, remind *D. aurantiacum* by having stalked sporangia with cartilaginous peridium and well-developed columella. However, they can be both distinguished by brown triple peridium rather than dull orange double peridium, close to areolate, and completely colorless capillitial threads (Geo, Rex, 1893; Novozhilov *et al.*, 2014).

The authors of the original description compared *Diderma aurantiacum* with *D. lucidum* Berk et Br. [ $\equiv$  *Leangium lucidum* (Berk. et Broome) E. Sheld.] and *D. miniatum* Nann.-Bremek. (Nannenga-Bremekamp, Yamamoto, 1990). Sporangia of both of these species are bright orange or scarlet and have well-developed, abundantly branched capillitium forming a reticulate structure. In addition, *D. lucidum* is characterized by a short, thin, black stalk, peridium that does not dehisce in a floriform manner forming curled “petals”, conical or slightly club-shaped columella, and larger spores — 13–15  $\mu\text{m}$  (Martin, Alexopoulos, 1969; Emoto, 1977; Ing, 1999). Sporangia of *D. miniatum* can be larger (about 2 mm tall and 1 mm diam.), have stout stalks filled with white crystalline lime, light orange conical columella reaching the center of sporangium, and spores evenly ornamented with small warts (Nannenga-Bremekamp, 1989; Lado *et al.*, 2019). Morphology of *D. aurantiacum* may be compared with *D. aurantiocolumellatum* Adamonyte, Seraoui et Michaud with deep yellow or orange lime in peridium. It is distinguished by always sessile sporangia and bright orange peridium, which crumbles away in segments together with attached capillitium threads leaving exposed columella (Adamonyte *et al.*, 2011).

### Phylogenetic study

A total of 29 new nucleotide sequences were generated for this study. The final dataset consisted of 64 specimens belonging to 27 morphological species of five genera. The concatenated alignment for ML and BI analyses included 64 nrSSU sequences

and 64 EF1 $\alpha$  sequences with 1380 sites, 609 distinct patterns, 24 singleton sites, and 847 constant (non-informative) sites in total. The topologies of ML and BI phylogenies were congruent and the clades that received high statistical support with UBS and PP were mostly identical.

Figure 4 shows the resulting two-gene phylogeny. The tree is rooted with species of *Lamproderma* (Lamprodermataceae, Physarales), being a basal clade to the order Physarales (Leontyev et al., 2019).

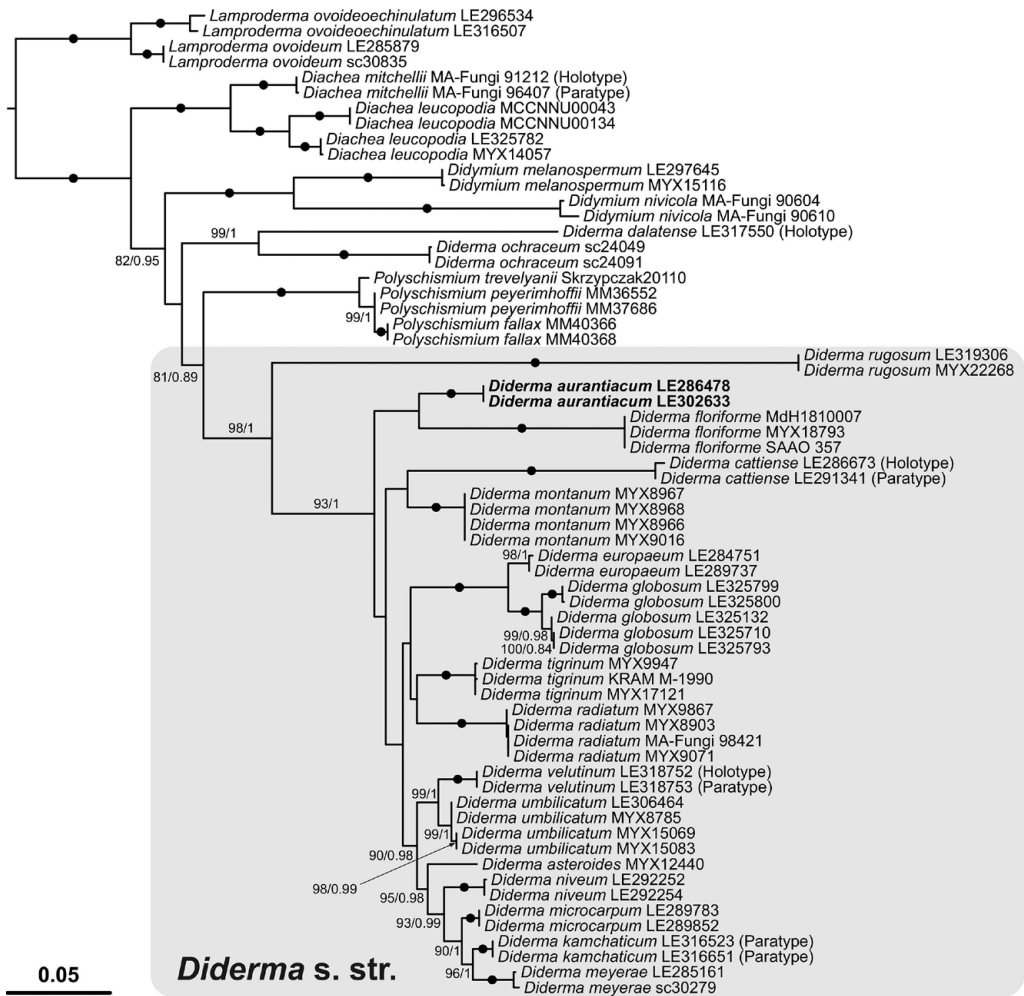


Fig. 4. Phylogenetic tree for species of *Diderma* and related genera, obtained from combined nrSSU and EF1 $\alpha$  sequences. Branch supports are shown only for UBS/PP  $\geq$  80/0.8; black dots indicate maximum supports in both analyses (UBS/PP = 100/1). Scale bar represent the mean number of nucleotide substitutions per site.

As it has been previously shown (Prikhodko *et al.*, 2023) that the genus *Diderma* in the traditional interpretation (Martin, Alexopoulos, 1969) is not monophyletic. *Diderma ochraceum* and *D. dalatense*, referred to subgenus *Leangium*, form an outer group relative to the newly erected genus *Polyschismium* (accommodating mostly the nivicolous species of the former genus *Lepidoderma*) and a clade named *Diderma* s. str., which includes the type species *Polyschismium trevelyanii* and *Diderma globosum*, respectively (Fig. 4; also see Prikhodko *et al.*, 2023). A distinctive feature of the members of the *Diderma* s. str. clade is the presence of a well-defined columella and mainly stalked sporangia. Notably, the presence of an eggshell-like peridium consisting of tightly packed lime granules is not a diagnostic feature for distinguishing the genus, as previously thought (Ronikier *et al.*, 2022; Prikhodko *et al.*, 2023).

The studied specimens of *Diderma aurantiacum* are nearly identical in partial nrSSU, mtSSU, and EF1 $\alpha$  sequences. Meanwhile, both specimens have different indels in COI sequences. Such differences are a good example of the fact that mitochondrial genes of myxomycetes can display a greater variability than classical nuclear markers and can be used in the detection of hidden biodiversity in Myxomycetes.

The topology of the ML-tree (Fig. 4) indicates the proximity of *Diderma aurantiacum* to *D. floriforme*, the type species of the former genus or subgenus *Leangium* (Fig. 2A–G), which is supported by the Bayesian analysis (UBS/PP = 67/0.97). As mentioned above, these species are indeed morphologically quite similar in stalked sporangia with a developed columella and petal-like dehiscence of the peridium. They mainly differ in peridium color, columella shape, and spore ornamentation, as well as in the nucleotide sequences of nrSSU and EF1 $\alpha$  (see Supplementary Material).

Despite the morphological similarity of some species previously attributed to the genus *Leangium* ( $\equiv$  *Diderma* subgen. *Leangium*) and allied species, including *Diderma asteroides*, *D. cattiense*, *D. floriforme*, *D. radiatum*, *D. rugosum*, *D. umbilicatum*, *D. velutinum*, and *Polyschismium trevelyanii*, the recognition of *Leangium* as a separate taxon (subgenus) is not justified. These species do not form an independent monophyletic group, but occupy an unresolved position next to *Diderma globosum* and other species of subgenus *Diderma*, which agrees with previously published data (Prikhodko *et al.*, 2023).

## Acknowledgments

We express our gratitude to the staff of the interdepartmental electron microscopy laboratory of the Faculty of Biology, MSU and personally to Nadezhda I. Kireeva for assisting with some specimens examined in the current study, Maria M. Gomzhina for organizing the work at the Mycological Herbarium of A. A. Jaczewskii Laboratory of Mycology and Phytopathology, All-Russian Institute of Plant Protection (LEP), and Nadezda A. Bortnikova for help with translation and valuable comments.

The molecular lab work of I. S. Prikhodko and Yu. K. Novozhilov was supported by the Ministry of Science and Higher Education of the Russian Federation (agreement № 075-15-2021-1056) and the state task “Biodiversity, ecology, structural and functional features of fungi and fungus-like protists” (BIN RAS, 122011900033-4),

they acknowledge the use of equipment of the Core Facility Center “Cell and Molecular Technologies in Plant Science” at the Komarov Botanical Institute of the Russian Academy of Sciences (BIN RAS, St. Petersburg). The field work of V. I. Gmshinskiy was funded by the Polistovsky Nature Reserve (project FEA – 1-22-66-3) and identification and study of specimens was carried out within the state assignment of the Ministry of Science and Higher Education of the Russian Federation (№ 075-15-2021-1396). For Martin Schnittler, laboratory work was in part supported by the German Research Foundation (DFG, grants RTG 2010, SCHN 1080/2-1).

## References

- Adamonyte G., Stephenson S. L., Michaud A., Seraoui E.-H., Meyer M., Novozhilov Y. K., Krivomaz T. 2011. Myxomycete species diversity on the island of La Réunion (Indian Ocean). *Nova Hedwigia* 92: 523–549. <https://doi.org/10.1127/0029-5035/2011/0092-0523>
- Emoto Y. 1977. *The Myxomycetes of Japan*. Tokyo: 263 p.
- Farr M. L. 1971. Two undescribed Myxomycetes from Argentina. *Mycologia* 63 (3): 634–639. <https://doi.org/10.1016/j.ympcv.2007.12.011>
- Fiore-Donno A. M., Meyer M., Baldauf S. L., Pawlowski J. 2008. Evolution of dark-spored *Myxomycetes* (slime-molds): molecules versus morphology. *Molecular Phylogenetics and Evolution* 46: 878–889. <https://doi.org/10.1111/j.1550-7408.2005.00032.x>
- Fiore-Donno A. M., Nikolaev S. I., Nelson M., Pawlowski J., Cavalier-Smith T., Baldauf S. L. 2010. Deep phylogeny and evolution of slime moulds (*Mycetozoa*). *Protist* 161: 55–70. <https://doi.org/10.1016/j.protis.2009.05.002>
- Fiore-Donno A. M., Novozhilov Y. K., Meyer M., Schnittler M. 2011. Genetic structure of two protist species (*Myxogastria*, *Amoebozoa*) suggests asexual reproduction in sexual amoebae. *PLoS ONE* 6(8): e22872. <https://doi.org/10.1371/journal.pone.0022872>
- Fiore-Donno A. M., Tice A. K., Brown M. W. 2019. A non-flagellated member of the *Myxogastria* and expansion of the *Echinosteliida*. *Journal of Eukaryotic Microbiology* 66: 538–544. <https://doi.org/10.1111/jeu.12694>
- Geo A., Rex M. D. 1893. New North American Myxomycetes. *Proceedings of the Academy of Natural Sciences of Philadelphia* 45(2): 364–372.
- Harakon Y., Li Y., Ooga S. 2005. Myxomycetes of the Kyushu University Forests. *Bulletin of the Kyushu University Forests* 86: 33–54. <https://doi.org/10.15017/14855>
- Hoang D. T., Chernomor O., von Haeseler A., Minh B. Q., Vinh L. S. 2018. UFBoot2: Improving the Ultrafast Bootstrap Approximation. *Molecular Biology and Evolution* 35(2): 518–522. <https://doi.org/10.1093/molbev/msx281>
- Huelsenbeck J. P., Ronquist F. 2001. MrBayes: Bayesian inference of phylogeny. *Bioinformatics* 17: 754–755. <https://doi.org/10.1093/bioinformatics/17.8.754>
- Ing B. 1999. *The myxomycetes of Britain and Ireland*. London: 374 p.
- Kalyaanamoorthy S., Minh B. Q., Wong T. K. F., von Haeseler A., Jermini L. S. 2017. ModelFinder: fast model selection for accurate phylogenetic estimates. *Nature Methods* 14: 587–589. <https://doi.org/10.1038/nmeth.4285>
- Katoh K., Standley D. M. 2013. MAFFT multiple sequence alignment software version 7: improvements in performance and usability. *Molecular Biology and Evolution* 30: 772–780. <https://doi.org/10.1093/molbev/mst010>
- Katoh K., Rozewicki J., Yamada K. D. 2019. MAFFT online service: multiple sequence alignment, interactive sequence choice and visualization. *Briefings in Bioinformatics* 20(4): 1160–1166. <https://doi.org/10.1093/bib/bbx108>

- Lado C. 2005–2023. An on line nomenclatural information system of Eumycetozoa. Real Jardín Botánico, CSIC. Madrid, Spain. <http://www.nomen.eumycetozoa.com> (Date of access: 15 I 2023).
- Lado C., Wrigley De Basanta D., Estrada-Torres A., Stephenson S. L., Treviño I. 2019. Diversity of Myxomycetes in arid zones of Peru part II: the cactus belt and transition zones. *Anales del Jardín Botánico de Madrid* 76 (2): e083. <https://doi.org/10.3989/ajbm.2520>
- Lado C., Treviño-Zevallos I., García-Martín J. M., Wrigley de Basanta D. 2022. *Diachea mitchellii*: a new myxomycete species from high elevation forests in the tropical Andes of Peru. *Mycologia* 114: 798–811. <https://doi.org/10.1080/00275514.2022.2072140>
- Leontyev D. V., Schnittler M., Stephenson S. L., Novozhilov Yu. K., Shchepin O. N. 2019. Towards a phylogenetic classification of the Myxomycetes. *Phytotaxa* 399(3): 209–238. <https://doi.org/10.11646/phytotaxa.399.3.5>
- Link H. F. 1809. Observationes in Ordines plantarum naturales I. Anandrarum ordines Epiphytas, Mucedines, Gastromycos et Fungos. *Der Gesellschaft Naturforschender Freunde zu Berlin* 3: 3–42.
- Lister A., Lister G. 1911. *A monograph of the Mycetozoa*. London: 302 p.
- Liu Q. S., Yan S. Z., Chen S. L. 2015. Further resolving the phylogeny of *Myxogastria* (slime molds) based on COI and SSU rRNA genes. *Genetika* 51: 46–53. <https://doi.org/10.7868/S0016675814110071>
- MacBride T. J. 1899. *The North American slime-moulds*. London: 269 p.
- Martin G. W., Alexopoulos C. J. 1969. *The Myxomycetes*. Iowa City: 561 p.
- Miller M. A., Pfeiffer W., Schwartz T. 2010. Creating the CIPRES Science Gateway for inference of large phylogenetic trees. *Gateway Computing Environments Workshop (GCE)*: 1–8. <https://doi.org/10.1109/GCE.2010.5676129>
- Nannenga-Bremekamp N. E. 1968. Notes on myxomycetes XVI. Remarks on some species of *Diderma*. *Proceedings of the Koninklijke Nederlandse Akademie van Wetenschappen. Ser. C, Biological and medical sciences* 71(2): 189–200.
- Nannenga-Bremekamp N. E. 1989. Notes on Myxomycetes XXIII. Seven new species of Myxomycetes. *Proceedings of the Koninklijke Nederlandse Akademie van Wetenschappen. Ser. C, Biological and medical sciences* 92(4): 505–515.
- Nannenga-Bremekamp N. E., Yamamoto Y. 1990. Additions to the Myxomycetes of Japan. *Proceedings of the Koninklijke Nederlandse Akademie van Wetenschappen. Ser. C, Biological and medical sciences* 93(3): 265–280.
- Nguyen L. T., Schmidt H. A., von Haeseler A., Minh B. Q. 2015. IQ-TREE: a fast and effective stochastic algorithm for estimating maximum-likelihood phylogenies. *Molecular Biology and Evolution* 32(1): 268–274. <https://doi.org/10.1093/molbev/msu300>
- Novozhilov Yu. K., Okun M. V., Erastova D. A., Shchepin O. N., Zemlyanskaya I. V., García-Carvajal E., Schnittler M. 2013. Description, culture and phylogenetic position of a new xerotolerant species of *Physarum*. *Mycologia* 105: 1535–1546. <https://doi.org/10.3852/12-284>
- Novozhilov Yu. K., Mitchell D. W., Okun M. V., Shchepin O. N. 2014. New species of *Diderma* from Vietnam. *Mycosphere* 5(4): 554–564. <https://doi.org/10.5943/mycosphere/5/4/8>
- Novozhilov Yu. K., Schnittler M., Erastova D. A., Shchepin O. N. 2017. Myxomycetes of the Sikhote Alin State Nature Biosphere Reserve (Far East, Russia). *Nova Hedwigia* 104(1–3): 183–209. [https://doi.org/10.1127/nova\\_hedwigia/2016/0394](https://doi.org/10.1127/nova_hedwigia/2016/0394)
- Novozhilov Yu. K., Prikhodko I. S., Shchepin O. N. 2019. A new species of *Diderma* from Bidoup Nui Ba National Park (southern Vietnam). *Protistology* 13: 126–132. <https://doi.org/10.21685/1680-0826-2019-13-3-2>
- Okonechnikov K., Golosova O., Fursov M., UGENE team. 2012. Unipro UGENE: a unified bioinformatics toolkit. *Bioinformatics* 28: 1166–1167. <https://doi.org/10.1093/bioinformatics/bts091>

- Person C. H. 1794. Dispositio methodica fungorum. *Neues Magazin für die Botanik* 1: 81–128.
- Poulain M., Meyer M., Bozonnet J. 2011. *Les Myxomycètes. Tome 1, guide de détermination*. Sévriér: 568 p.
- Prikhodko I. S., Shchepin O. N., Bortnikova N. A., Novozhilov Yu. K., Gmshinskiy V. I., Moreno G., López-Villalba Á., Stephenson S. L., Schnittler M. 2023. A three-gene phylogeny supports taxonomic rearrangements in the family *Didymiaceae* (*Myxomycetes*). *Mycological Progress* 22: 11. <https://doi.org/10.1007/s11557-022-01858-1>
- Rambaut A., Drummond A. J., Xie D., Baele G., Suchard M. A. 2018. Posterior summarization in Bayesian phylogenetics using Tracer 1.7. *Systematic Biology* 67: 901–904. <https://doi.org/10.1093/sysbio/syy032>
- Ronikier A., Janik P., de Haan M., Kuhnt A., Zankowicz M. 2022. Importance of type specimen study for understanding genus boundaries – taxonomic clarifications in *Lepidoderma* based on integrative taxonomy approach leading to resurrection of the old genus *Polyschismium*. *Mycologia* 114(6): 1008–1021. <https://doi.org/10.1080/00275514.2022.2109914>
- Vaidya G., Lohman D. J., Meier R. 2011. SequenceMatrix: concatenation software for the fast assembly of multi-gene datasets with character set and codon information. *Cladistics* 27: 171–180. <https://doi.org/10.1111/j.1096-0031.2010.00329.x>
- Yamamoto Y. 1998. *The myxomycete biota of Japan*. Tokyo: 700 p.
- Yano M., Yano K., Yamamoto Y., Orihara T. 2017. Myxomycete biota of Izu Peninsula, Central Japan. *Bulletin of the Kanagawa Prefectural Museum, Natural Science* 46: 25–38.